Molecular Pharmacology Fast Forward. Published on July 16, 2012 as doi: 10.1124/mol.112.078683

MOL#78683

Title page

Efficient binding of 4/7 α-conotoxins to nicotinic α4β2 receptors is prevented by R185 and P195 in the α4 subunit

Mirko Beissner, Sébastien Dutertre, Rudolf Schemm, Timm Danker, Annett Sporning, Helmut Grubmüller, and Annette Nicke

Max Planck Institute for Brain Research, Dept. of Neurochemistry, Deutschordenstr. 46, 60528 Frankfurt, Germany (M. B. and A.N.)

Institute for Molecular Bioscience, University of Queensland, Brisbane, QLD 4072, Australia (S. D.)

Max Planck Institute for Biophysical Chemistry, Dept. of Theoretical and Computational Biophysics, Am Faßberg 11, 37077 Göttingen, Germany (R. S. and H. G.)

NMI Technologie Transfer GmbH, Markwiesenstrasse 55, 72770 Reutlingen, Germany (T. D.)

Max Planck Institute for Experimental Medicine, Dept. of Molecular Biology of Neuronal Signals, Hermann Rein-Str. 3, 37075 Göttingen, Germany (A. S. and A. N.)

Molecular Pharmacology Fast Forward. Published on July 16, 2012 as DOI: 10.1124/mol.112.078683
This article has not been copyedited and formatted. The final version may differ from this version.

Running Title Page

Running title: *α-conotoxin binding to α4β2 receptors*

To whom correspondence should be addressed:

Dr. Annette Nicke

Max Planck Institute for Experimental Medicine, Hermann-Rein-Str. 3, 37075 Göttingen, Germany

Phone: +495513899 420, Fax: +495513899644, e-mail: anicke@gwdg.de

Number of text pages 25

Number of tables 3

Number of figures 5

Number of references 36

Number of words

Abstract 163

Introduction 452

Discussion 1118

Abbreviations: ACh, acetylcholine; AChBP, acetylcholine binding protein; EM, electron microscopy; HEPES, 2-(4-(2-Hydroxyethyl)- 1-piperazinyl)-ethansulfonsäure; LBD, ligand binding domain; MD, molecular dynamics; nAChR, nicotinic acetylcholine receptor; rmsd, root mean square deviation; TEVC, two-electrode voltage-clamp

Molecular Pharmacology Fast Forward. Published on July 16, 2012 as DOI: 10.1124/mol.112.078683
This article has not been copyedited and formatted. The final version may differ from this version.

Abstract

α-Conotoxins are subtype-selective nAChR antagonists. While potent α3β2 nAChR-selective α-contoxins have been identified, currently characterized α-conotoxins show no or only weak affinity for α4β2 nAChRs, which are besides α7 receptors the most abundant nAChRs in the mammalian brain. To identify the determinants responsible for this difference, we substituted selected amino acid residues in the ligand binding domain of the α4 subunit by the corresponding residues in the α3 subunit. Two-electrode voltage-clamp analysis of these mutants revealed increased affinity of α-conotoxins MII, TxIA, and [A10L]TxIA at the α4(R185I)β2 receptor. Conversely, α-conotoxin potency was reduced at the reverse α3(I186R)β2 mutant. Replacement of α4R185 by alanine, glutamate, and lysine demonstrated that a positive charge in this position prevents α-conotoxin binding. Combination of the R185I mutation with a P195Q mutation outside the binding site but in loop C completely transferred high α-conotoxin potency to the α4β2 receptor. Molecular dynamics simulations of homology models with docked α-conotoxin indicate that these residues control access to the α-conotoxin binding site.

Molecular Pharmacology Fast Forward. Published on July 16, 2012 as DOI: 10.1124/mol.112.078683
This article has not been copyedited and formatted. The final version may differ from this version.

Introduction

Neuronal nicotinic acetylcholine receptors (nAChRs) constitute a diverse family of pentameric ion channels that are formed by variable assembly from at least eight α- and three β-subunits (α2-α6, α7, α9, α10, and β2-β4). The α2, α3, α4, and α6 subunits require coexpression of at least one β (β2 or β4) subunit to form functional channels. The ACh binding site has been located at the interface between an α-subunit (+face) and an adjacent β subunit (– face), or, in the case of the α7, α9, and α10 subunits, another α subunit (–face). The "structural" α5 and β3 subunits appear unable to form functional channels in any pairwise combination but contribute to the diversity of pentameric αβ combinations in channels with three or four different subunits (Gotti et al., 2009).

The nicotinic a4b2* subtype (* denotes the possible presence of additional subunits) is the most abundant heteromeric nicotinic receptor in the brain. It plays a role in cognitive processes and represents a therapeutic target for smoking cessation as well as for the treatment of pain and a variety of neurological disorders such as Alzheimers´s and Parkinson´s diseases, depression, and attention deficit disorders (Taly et al., 2009). α-Conotoxins, a family of small disulfide peptides isolated from the venom of predatory marine snails, are highly selective nAChR antagonists that bind at the intersubunit agonist binding site and thereby discriminate between closely related nAChR subtypes. They have proven to be useful pharmacological tools to localize nAChR subtypes and to investigate their specific subunit composition and physiological functions (Nicke et al., 2004). The 4/7 α-conotoxins represent the largest α-conotoxin subfamily. Most of the identified 4/7 α-conotoxins target α7 and/or α3β2* nAChRs with low nanomolar potency. Equally potent 4/7 α-conotoxins with selectivity for the α6β2 receptor (which is

Molecular Pharmacology Fast Forward. Published on July 16, 2012 as DOI: 10.1124/mol.112.078683
This article has not been copyedited and formatted. The final version may differ from this version.

closely related to the α3β2 subtype) have been isolated from crude venom or have been generated by modification of the α3β2- and α6β2-selective α-conotoxin MII (Nicke et al., 2004; Azam and McIntosh, 2009). So far, no conotoxin has been identified that selectively targets α4β2 nAChRs and only a few α-conotoxins, MII (Cartier et al., 1996), GID (Nicke et al., 2003), GIC (McIntosh et al., 2002), and AnIB (Loughnan et al., 2004), have been shown to block this receptor at all, although at high nanomolar or micromolar concentrations.

Given the abundance of α4β2* receptors in the brain and their importance as drug targets, potent and specific pharmacological tools for this receptor are needed. Here we show that an arginine residue in position 185 and a proline residue in position 195 of the α4 subunit prevent efficient α-conotoxin binding. Our data provide molecular determinants of subtype selectivity and thus represent a basis for the design of optimized α-conotoxins with tailored subtype selectivity.

Material and Methods

Homology modelling and molecular dynamics simulations – The dimeric homology model of the ligand-binding domain (LDB) of the α4β2 nAChRs was based on the muscle-type nAChR (Unwin, 2005). This model was generated with Modeller9v8-1 (Sali and Blundell, 1993) using two alpha subunits of the refined EM structure of the *Torpedo marmorata* nAChR polypeptide chains (pdb code 2BG9). These show a considerably higher homology to the α4- and β2 nAChR subunits than that of the AChBP. Although the structural assignment might be critical due to the resolution of only 4 Å of 2BG9, a recently published structure of the Glu-gated chloride channel GluCl (3.3 A, pdb code

Molecular Pharmacology Fast Forward. Published on July 16, 2012 as DOI: 10.1124/mol.112.078683
This article has not been copyedited and formatted. The final version may differ from this version.

3RIF) (Hibbs & Gouaux, 2011) and the common alignment of the loop C region support its reliability. For a comparison of this models with a previously generated AChBP-based model in terms of structural changes of loop C (rmsd), see Supplemental Fig.2.

Because we intended to measure binding energies of conotoxins, which correlate with their ability to inhibit AChRs and not gating movements, we decided to restrict to a dimeric model for docking and MD studies instead of using a full receptor or LBD model. This was also more feasible in terms of simulation times needed for statistcal analysis. All molecular dynamics (MD) simulations were performed using Gromacs (version 4.0.7 and 4.5.5) (Hess et al., 2008) and the amber03 force field (Duan et al., 2003). Dimeric wild-type and mutant α4β2 ligand binding domains with α-conotoxin [A10L]TxIA were generated with the capping groups ace and nme (Sybyl 8.0.1, Tripos St Louis, MO, USA). The proteins were placed in a rectangular box filled with tip4p water (Mahoney and Jorgensen, 2000) and Na^+ and Cl^- ions (0.15 M) and, after energy minimization, subjected to 50 ns MD runs whereby position restraints of 10 kJ/(mol*nm2) were set on the protein atoms (without H) except for loop C (Y182-I197) and the conotoxin. From the resulting trajectories distances and binding energies (sum of short range Coulomb and Lennard-Jones energies) of the α-conotoxin to the α4 and β2 subunits, respectively were calculated. For this purpose, from each trajectory 20.000 frames (10-50 ns) were used for analysis. The first 10 ns from each trajectory were discarded to minimize equilibration effects. For each value, 8 to 10 trajectories were generated, and distances and interaction energies were averaged (Fig. 5). To determine the significance of the overall trend for stronger binding enthalpies for 0<1<2<3, a Bayesian analysis (see supplemental information) for linear fit functions $y=m*x+b$ was

Molecular Pharmacology Fast Forward. Published on July 16, 2012 as DOI: 10.1124/mol.112.078683
This article has not been copyedited and formatted. The final version may differ from this version.

carried out with *x*=[0,1,2,3] for [wt, P195Q, R185I, P195Q/R185I], respectively, assuming an unbiased a priori distribution for the slope *m* and the offset *b*. For the resulting a posteriori probability distribution *p(m)*, integrated over all offsets, a probability of 0.9986 is found for negative *m*, implying a significance level of 0.14%.

Peptide sources – α-MII was obtained from Tocris. α-TxIA and α-[A10L]TxIA were synthesized using Boc chemistry with in situ neutralization protocols as previously described (Dutertre et al., 2007).

Electrophysiological measurements – nAChR cDNAs were provided by J. Patrick (Baylor College of Medicine, Houston, TX, USA) and subcloned into the oocyte expression vector pNKS2. Site-directed mutagenesis was performed with the QuikChange mutagenesis Kit (Stratagene, La Jolla, CA, USA). Primer synthesis and sequencing was performed by MWG Biotech AG (Ebersberg, Germany). cRNA was synthesized with the SP6 mMessage mMachine kit (Ambion, Austin, TX, USA) and *Xenopus laevis* (Nasco International, Fort Atkinson, WI, USA) oocytes were injected with 50 nl aliquots of cRNA (0.5 mg/ml), either manually or using the Roboinject robot (MCS, Reutlingen, Germany). nAChR subunits were mixed in the ratios 1:1 (α3:β2) or 5:1 (α4:β2).

Antagonist dose response curves were measured as described (Dutertre et al., 2005) in ND96 (96 mM NaCl, 2 mM KCl, 1 mM $CaCl_2$, 1 mM $MgCl_2$, and 5 mM Hepes at pH 7.4). Shortly, current responses to acetylcholine were recorded at –70 mV using a Turbo Tec 05X Amplifier (NPI Electronic, Tamm, Germany) and Cell Works software. A standard concentrations of 100 μM ACh was used to keep the data comparable with

Molecular Pharmacology Fast Forward. Published on July 16, 2012 as DOI: 10.1124/mol.112.078683
This article has not been copyedited and formatted. The final version may differ from this version.

previous studies. However, comparison of the inhibition of the α3β2 subtype by 3 nM [A10L]TxIA at 30, 100, and 300 μM (~EC_{50} for wild-type α3β2) ACh showed no significant differences in the toxin effect suggesting that the ACh concentration is not critical under the described conditions (preapplication of toxin). A fast and reproducible solution exchange (< 300 ms) was achieved with a 50 μl funnel-shaped oocyte chamber combined with a fast solution flow (~150 μl/s) fed through a custom-made manifold mounted immediately above the oocyte. Agonist pulses were applied for 2 s at 4 min intervals. Peptides were applied for three minutes in a static bath. IC_{50} values were calculated from a non-linear fit of the Hill equation to the data (Prism GraphPad v 4.0, San Diego, CA). Data are presented as mean ± S.E. from at least 4 experiments.

Agonist dose response curves for ACh were recorded in Ca^{2+}-free Buffer (96 mM NaCl, 2 mM KCl, 1 mM MgSO4, 5 mM HEPES, pH 7.4), supplemented with 0.5 μM Atropine, using the Roboocyte platform (MCS, Reutlingen, Germany (Leisgen et al., 2007)) (Pehl et al., 2004) or the conventional TEVC set up described above. Oocytes were clamped at -60 or -70 mV. 2 or 3 second pulses of the indicated agonist concentrations were applied in alternation with a 200 (Robocyte) or 300 μM reference concentration to account for receptor run down. Current responses to ACh were calculated in relation to the reference pulses and the normalized dose response data were fitted to the 4 parametric Hill equation using Prism GraphPad. In cases where the Hill coefficient could not be accurately determined, it was constrained to a range from 0 to 2.

Molecular Pharmacology Fast Forward. Published on July 16, 2012 as DOI: 10.1124/mol.112.078683
This article has not been copyedited and formatted. The final version may differ from this version.

Results

Generation and functional expression of mutant α4β2 nAChRs – The α4 and α3 nAChR subunits have 61.84 % sequence identity in their ligand binding domain. From the sequence alignment of these two sequences (Fig. 1), we selected four amino acid residues located in the proposed conotoxin binding site that differed between the α4 subunit and the α3 subunit. Using site directed mutagenesis, these α4 residues were replaced with the respective α3 residues: T147S, R185I, E188N, and A191E. To confirm that the mutations do not markedly alter the functional properties of the receptors, wt and mutant α4 subunits were coexpressed with the β2 subunits in *Xenopus laevis* oocytes and dose response curves for ACh were recorded using the robocyte automated two-electrode voltage clamp system (Fig. 2). This automated screen revealed that all single point mutants were functionally expressed and their EC_{50} values for ACh were in the same order of magnitude as that of the wt receptor (Table 1).

The α4R185I mutation enables efficient binding of α-conotoxins MII, TxIA and [A10L]TxIA to the α4β2 receptor – α-Conotoxin MII blocks heterologously expressed α3β2 and α6β2* nAChRs with low nanomolar potency (IC_{50}: 0.5-8 nM and 0.4 nM, respectively (Cartier et al., 1996; Dowell et al., 2003; Harvey et al., 1997; Kaiser et al., 1998; McIntosh et al., 2004)). Because it also blocks α4β2 nAChRs at about 100-1000-fold higher concentrations (IC_{50}: 430-550 nM (Cartier et al., 1996)), we initially determined dose-response relationships of α-conotoxin MII on wt and mutant α4β2 nAChRs to test if any of the mutations in the α4 subunit improved its affinity. As shown in Fig. 3A and table 2, the α4R185I exchange caused a more than 10-fold decrease of the IC_{50} value (193 nM) in comparison to the wt α4β2 nAChR (3293 nM) while all other

Molecular Pharmacology Fast Forward. Published on July 16, 2012 as DOI: 10.1124/mol.112.078683
This article has not been copyedited and formatted. The final version may differ from this version.

mutations did not significantly alter the potency of MII. To examine whether these findings were specific for α-conotoxin MII we next investigated the dose-response relationships of α-conotoxins TxIA and [A10L]TxIA. As previously determined (Dutertre et al., 2007), TxIA and [A10L]TxIA have similar potency compared to MII on α3β2 nAChRs (IC_{50}: 2 and 3.6 nM, respectively) but in contrast to MII, they also block homomeric α7 nAChR with IC_{50} values of 390 nM and 39 nM, respectively, and show no affinity for the α4β2 receptor at concentrations up to 10 μM (Dutertre et al., 2007). Both analogues have comparably little sequence identity with MII apart from the residues that are generally conserved in most 4/7α-conotoxins such as the four cysteine residues, G1, and P6 (Table 3). As seen with MII, no significant improvement of affinity was caused by the T147S, E188N, and A191E mutations in the α4 subunit while the effect of the R185I mutation was even stronger than for MII with a more than 1000-fold affinity increase, which made TxIA a potent blocker (IC_{50}: 18 nM) at this mutant (Fig. 3B). Likewise, the [A10L]TxIA-analogue was rendered into an efficient antagonist (IC_{50} 123 nM) at the α4(R185I)β2 mutant (Fig. 3D).

The α3I186R mutation impairs binding of α-conotoxins MII, TxIA, and [A10L]TxIA to the α3β2 receptor – R185 lies in a stretch of 15 amino acids (174-188) in the β9 strand preceding the critical cysteine pair that forms a vicinal disulfide bridge at the tip of loop C, which covers the intersubunit binding site (Fig. 1). These residues are highly variable between the α3 and α4 subunits, which might result in different backbone conformations of the loop C and consequently generally different dimensions or accessibility of the conotoxin binding sites. However, our results with MII demonstrate that the α4β2 binding site can principally accommodate α-conotoxins but that R185

Molecular Pharmacology Fast Forward. Published on July 16, 2012 as DOI: 10.1124/mol.112.078683
This article has not been copyedited and formatted. The final version may differ from this version.

might specifically clash with one or more residues in the α-conotoxins and thus prevent or impair their high affinity binding. To further investigate the specific role of the side chain in this position we replaced the equivalent isoleucine residue in the α3β2 receptor by an arginine residue. This I186R exchange in the α3 subunit caused a more than 10-fold decrease in the affinity of MII (IC_{50}: 58 nM) and a 30-fold decrease in the affinity of TxIA (IC_{50}: 60 nM) and [A10L]TxIA (IC_{50} 77 nM). Thus, TxIA was even slightly more potent at the α4(R185I)β2 receptor than at the α3(I186R)β2 receptor. These results are in agreement with our assumption that R185 specifically interacts with α-conotoxin binding.

α-conotoxin binding to α4β2 receptors is prevented by a positively charged residue in position 185 of the α4 subunit – Next we exchanged R185 in the α4 subunit by alanine, lysine, and glutamate to determine if a positive charge is required to prevent α-conotoxin binding or if this is due to a steric effect of the bulky arginine side chain. As shown in Fig. 3D, replacement of arginine by alanine or the negatively charged glutamate caused comparable potency increases of [A10L]TxIA as the substitution by isoleucine with IC_{50} values of 372 nM and 118 nM, respectively. In contrast, [A10L]TxIA was inactive at the α4(R185K)β2 mutant. Together with the fact that the substitution by the negatively charged glutamate resulted in a 3-fold lower IC_{50} value than substitution by the small alanine, this suggests that a positive charge in position 185 of the α subunit prevents α-conotoxin-binding.

An additional α4P195Q mutation completely transfers low nanomolar potency of [A10L]TxIA to the α4β2 receptor – The α-conotoxin potencies achieved at the α4R185Iβ2 receptor are still in the medium to high (20 – 200 nM) nanomolar range. In

Molecular Pharmacology Fast Forward. Published on July 16, 2012 as DOI: 10.1124/mol.112.078683
This article has not been copyedited and formatted. The final version may differ from this version.

contrast, low to subnanomolar potencies are usually achieved at α3β2 and the closely related α6β2 subtype or the homomeric α7 subtype. Based on sequence alignment and homology modeling, we hypothesized that proline 195 could constitute the remaining obstacle (Fig. 1). Although it does not directly face the α-conotoxin binding site, it might disturb the binding by structurally altering the loop C. Indeed, replacement of α4P195 by the homologous glutamine residue found in the α3 subunit rendered [A10L]TxIA active at this receptor (IC_{50}: 707 nM). In combination with the R185I substitution, the P195Q mutation caused an additional 40-fold increase in the potency of [A10L]TxIA and rendered this mutant α4β2 receptor equally sensitive (IC_{50}: 3.2 nM) to [A10L]TxIA as the α3β2 subtype. Interestingly, the R185I/P195Q double exchange also significantly increased the sensitivity to ACh as determined by both automated and conventional analysis of DRCs (Table 1, Fig. 2).

Probing the binding mode of [A10L]TxIA at the α4β2 receptor – We have previously identified several mutants in the β2 subunit that improve the efficiency of conotoxins with a long side chain in position 10 to block the α3β2 receptor (Dutertre et al., 2005). We deduced from these studies that the first loop of α-conotoxins (residues 4-7) faces towards the α-subunit while the second loop (residues 9-15) interacts with the β subunit. This binding mode is in good agreement with co-crystallization studies of the acetylcholine binding protein and was further refined in subsequent functional studies (Celie et al., 2005) (Dutertre et al., 2007). To test if a principally similar binding mode was preserved in the α4R185Iβ2 mutant, we combined in analogous experiments the α4R185I subunit with the previously identified β2V109G mutant (Dutertre et al., 2005). Combination of these subunits caused an additional potency increase of [A10L]TxIA that

Molecular Pharmacology Fast Forward. Published on July 16, 2012 as DOI: 10.1124/mol.112.078683
This article has not been copyedited and formatted. The final version may differ from this version.

was at least 20-fold higher (IC_{50} 6,6 nM) than for each single mutation in combination with the respective wt-subunit (IC_{50}:123 nM and 213 nM, respectively, Fig. 3E, Table 2). Since we have previously found that the β2V109G mutation causes a potency increase of α-conotoxins with a long side chain in position 10 in combination with both wt-α3 and wt-α4 subunits (Dutertre et al., 2005), we suggest that this interaction with the β2(V109G) subunit is preserved in a similar way if combined with the α4(R185I) subunit. Consequently, the binding mode should not be different from what we have determined for the α3β2 receptor (Dutertre et al., 2005) and the α4 subunit likely interacts with the N-terminus of the α-conotoxin.

Computational studies of α-conotoxin binding mode at α4β2 receptors – Next, we placed [A10L]TxIA in the binding pocket of a α4β2 homology model in the same position where it was co-crystallised with AChBP (Dutertre et al., 2007). However, this procedure failed to identify a direct interaction of α4R185 with any conotoxin residue or with the conotoxin backbone (Fig. 4A). We therefore performed docking studies on a homology model based on the refined structure of the *Torpedo marmorata* nAChR (Unwin, 2005) α4 subunit (Fig. 4B). Remarkably, these docking simulations revealed an interaction of α4R185 with the arginine residue in position 5 of the conotoxins (Supplemental Figures 1A and 2). In addition, MD simulations revealed a weaker binding of conotoxin [A10L]TxIA at the wt proteins (Fig.4 C,D,E). In contrast, the same MD simulations run with the R185I mutation allow the conotoxin to bind deeper in its binding pocket (Fig. 4C, E). In addition, the P195Q substitution results in a greater flexibility of loop C, enabling a more peripheral position of the critical R185 residue that likewise allows a closer contact to the conotoxin (Fig. 4D, 5A). In case of the R185I/P195Q

Molecular Pharmacology Fast Forward. Published on July 16, 2012 as DOI: 10.1124/mol.112.078683
This article has not been copyedited and formatted. The final version may differ from this version.

double mutation, both effects lead to a further improved positioning of the conotoxin (Fig.4E, Supplemental Fig. 1B). However, no significant correlation between distance and conotoxin binding enthalpies is seen (Fig. 5A and B). For example, the conotoxin - β2 subunit distances remain between 1.5 and 1.6 nm, although the respective energies decrease implying stronger binding. Apparently, the different binding enthalpies are not explained by the distances between [A10L]TxIA and the β2 subunit. We also investigated the involvement of loop C - conotoxin interaction in the measured overall binding energies. However, the results for the different protein/conotoxin combinations (Supplental Fig. 3) do not strictly correlate with the calculated binding energies (Fig. 5). Consequently, we cannot ascribe the found conotoxin - protein interactions to the respective conotoxin - loop C residue interactions solely. Similarly, single fluctuations of loop C residues seem to be independent of the actual mutation state (Supplemental Fig 4). Nevertheless, analysis of structural changes (rmsd) during MD to estimate the contribution of loops C to conotoxin binding showed that R185 has the largest influence on loop C conformation (Supplemental Fig. 2).

While no significant binding enthalpy difference is seen for the P195Q mutation, the binding enthalpy is significantly stronger than in the wt for both the R185I mutant and the P/R double mutant (Fig. 5B). Moreover, an overall trend to stronger binding enthalpies of [A10L]TxIA with wt < P195Q < R185I < P195Q/R185I is seen at a significance level of 5×10^{-4} and reflects the results obtained in functional experiments (Fig. 5B).

Molecular Pharmacology Fast Forward. Published on July 16, 2012 as DOI: 10.1124/mol.112.078683
This article has not been copyedited and formatted. The final version may differ from this version.

Discussion

In this study, we have identified two amino acid residues, R185 and P195, in the α4 nicotinic receptor subunit that, if replaced by the corresponding residues in the α3 subunit, completely transferred the low nanomolar potency of α-conotoxin [A10L]TxIA to the α4β2 subtype which is otherwise insensitive to this toxin. Replacement of R185 by isoleucine resulted in a 10-fold (MII) up to at least 1000-fold (TxIA and [A10L]TxIA) enhanced potency of different 4/7 α-conotoxins at the α4β2 receptor subtype. Replacement of the corresponding I186 residue in the α3 subunit by an arginine residue reduced the potency of these conotoxins at the α3β2 receptor more than 10-fold. These findings are in good agreement with previous studies which demonstrated the importance of these two residues (Harvey et al., 1997) for MII and PnIA binding to the α3β2 receptor by replacing them with the homologous residues (K and P, respectively) from the conotoxin-insensitive α2 subunit (Everhart et al., 2003). Here, we further demonstrate that replacement of α4R185 by the smaller alanine or a negatively charged glutamate but not by a positively charged lysine enhanced affinity for of the α4β2 receptor for [A10L]TxIA. We conclude from these data, that a positive charge in this position specifically prevents high affinity binding of most conotoxins to the α4β2 nicotinic receptor and thus represents a major determinant for subtype selectivity. Since arginine and lysine are both very bulky residues, a steric interaction rather than a charge effect of α4R185 cannot be excluded and could explain the lack of activity of 4/7 α-conotoxins that carry a non-charged leucine residue in position 5 (such as PnIA and PnIB). In support of a charge effect, however, the identified α-conotoxins that show low activity at

Molecular Pharmacology Fast Forward. Published on July 16, 2012 as DOI: 10.1124/mol.112.078683
This article has not been copyedited and formatted. The final version may differ from this version.

the α4β2 receptor (MII, GID, GIC, and AnIB), have a neutral asparagine residue or an only partially protonated (at pH 7.4) histidine residue in this position.

The strong effect of the α4(R185I/P195Q) double mutation on the EC_{50} value for ACh might indicate that the combination of these mutations also produces an improved binding and/or gating efficiency of ACh. Alternatively, this mutation could disturb the expression of correctly folded α4 subunits and result in a reduced α4:β2 subunit ratio which has been demonstrated to produce α4β2 receptor stoichiometries with high affinity for ACh (Zwart and Vijverberg, 1998). The latter idea is supported by the fact that a decrease in the ratio of injected α4(P195Q):β RNA resulted in a reduced expression of functional receptors that showed a decreased EC_{50} value for ACh (results not shown).

Homology models as prediction tools – Initial visualisation of the complex receptor-conotoxin using a homology model based on the homomeric AChBP (Dutertre et al, 2007), failed to reveal a direct interaction that would prevent α-conotoxin binding (Fig. 4A and Supplemental Fig. 2). However, molecular dynamics and docking studies with [A10L]TxIA on a refined α4β2 homology model based on the *Torpedo marmorata* nAChR demostrated that the α4R185/conotoxin R5 interaction weakens the conotoxin binding suggesting that this vertebrate receptor, despite the lower resolution of its structure (4Å compared to 2.7Å for the AChBP structure), represents a more suitable template to generate rat α4β2 homology models. Nonetheless, a recent crystallization study on a soluble α7/AChBP chimera (Li et al.) that contains the loop C of the human α7 receptor with a similar loop C architecture and side chain positioning as our AChBP model supports the usefulness of this widely used model. Interestingly, loop C of the α7

Molecular Pharmacology Fast Forward. Published on July 16, 2012 as DOI: 10.1124/mol.112.078683
This article has not been copyedited and formatted. The final version may differ from this version.

receptor also contains R and P residues in homologous positions to the α4 subunit. Yet the α-conotoxins tested in our study were previously shown to efficiently block the α7 receptor with IC_{50} values of 39 nM ([A10L]TxIA), 100 nM (MII), and 392 nM (TxIA) (Cartier et al., 1996; Dutertre et al., 2007) and several α-conotoxins with even higher potencies at this receptor have been identified. This is in contrast to the strong effect of these residues in our functional studies and the poor affinity of all identified α-conotoxins at the α4β2 receptor. A possible explanation for this discrepancy could lie in the heteromeric nature of the α4β2 and α3β2 ligand binding sites which might have a different architecture and for which the heteromeric torpedo nAChR might provide a better template than the homomeric α7 and AChBP binding sites. In support of this, our MD simulations on a *Torpedo* nAChR-based model reproduced the rank order of potency of the conotoxin [A10L]TxIA on the different α4β2 mutants. A very recent study demonstrated that the homologous positions in the α6 subunit (I188 and T198) confer selectivity of α-conotoxin BuIA for this subunit (Kim and McIntosh, 2012). A direct interaction between BuIA and I188 could not be identified in their model of the complex and it was suggested that alterations in the loop C structure account for the potency differences of the conotoxin, a conclusion also supported by our MD simulation results.

Design of optimized α-conotoxins – α-conotoxins are important pharmacological tools that cannot only discriminate between distinct nicotinic receptor subtypes but are also able to differentiate between non-equivalent binding sites within the same heteromeric receptor (for a recent review see (Tsetlin et al., 2009)). Radioactively labelled or fluorescent α-conotoxins can help receptor localization (Hone et al.; Whiteaker et al., 2008) and α-conotoxins have the potential to be developed into novel

Molecular Pharmacology Fast Forward. Published on July 16, 2012 as DOI: 10.1124/mol.112.078683
This article has not been copyedited and formatted. The final version may differ from this version.

drugs (Olivera et al., 2008). So far, natural α-conotoxins with selectivity for the following neuronal nicotinic receptor subtypes have been identified: α3β2 and α6-containing nAChRs (MII), α9α10 nAChRs (RgIA), and α7 and α3β2 nAChRs (ImI) (Ellison et al., 2008; Ellison et al., 2004; McIntosh et al., 2004). The subtype selectivity of several α-conotoxins could be further optimized yielding analogues that are able to differentiate even between closely related nicotinic receptor subtypes. These include α-conotoxins with selectivity for α6-containing nAChRs (MII[S4A;E11A;L15A]), α6β4* nAChRs (BuIA[T5A;P6O], and α7 nAChRs (ArIB[V11L;V16D]) (Azam et al., 2010; Azam et al., 2008; Whiteaker et al., 2007). Apparently, conotoxins selective for mammalian α4β2 interfaces have not evolved in cone snails or up to now escaped discovery. α4β2-selective α-conotoxins would have the potential to differentiate not only between α4β2 and other nicotinic receptor subtypes but could potentially help to identify multiple α4β2* receptor assemblies which represents an important task in view of their variety in the CNS. In further studies, it is crucial to determine if α-conotoxins can be designed that are able to bind with high affinity to the α4β2 binding site or if this requires peptides with different backbone folds.

In conclusion, our study identified an important determinant of subtype selectivity between α3β2 and α4β2 nAChRs and indicates that α-conotoxins have substantially different binding modes at homomeric α7 and heteromeric α4β2 and α3β2 receptors. This information provides an essential basis and important caveat for further modelling and mutagenesis studies.

Molecular Pharmacology Fast Forward. Published on July 16, 2012 as DOI: 10.1124/mol.112.078683
This article has not been copyedited and formatted. The final version may differ from this version.

Acknowledgements

We thank Christiane Arnold for initial mutant generation and Conny Neblung for technical assistance.

Authorship Contributions

Participated in research design: Nicke, Dutertre

Conducted experiments: Beissner, Danker, Sporning, Nicke, Dutertre, Schemm

Contributed new reagents or analytic tools: Dutertre

Performed data analysis: Nicke, Danker, Schemm, Beissner, Grubmüller, Dutertre

Wrote or contributed to the writing of the manuscript: Nicke, Dutertre, Schemm, Grubmüller

References

Azam L, Maskos U, Changeux JP, Dowell CD, Christensen S, De Biasi M and McIntosh JM (2010) alpha-Conotoxin BuIA[T5A;P6O]: a novel ligand that discriminates between alpha6beta4 and alpha6beta2 nicotinic acetylcholine receptors and blocks nicotine-stimulated norepinephrine release. *FASEB J* **24**(12):5113-5123.

Azam L and McIntosh JM (2009) Alpha-conotoxins as pharmacological probes of nicotinic acetylcholine receptors. *Acta Pharmacol Sin* **30**(6):771-783.

Azam L, Yoshikami D and McIntosh JM (2008) Amino acid residues that confer high selectivity of the alpha6 nicotinic acetylcholine receptor subunit to alpha-conotoxin MII[S4A,E11A,L15A]. *J Biol Chem* **283**(17):11625-11632.

Cartier GE, Yoshikami D, Gray WR, Luo S, Olivera BM and McIntosh JM (1996) A new alpha-conotoxin which targets alpha3beta2 nicotinic acetylcholine receptors. *J Biol Chem* **271**(13):7522-7528.

Celie PH, Kasheverov IE, Mordvintsev DY, Hogg RC, van Nierop P, van Elk R, van Rossum-Fikkert SE, Zhmak MN, Bertrand D, Tsetlin V, Sixma TK and Smit AB (2005) Crystal structure of nicotinic acetylcholine receptor homolog AChBP in complex with an alpha-conotoxin PnIA variant. *Nat Struct Mol Biol* **12**(7):582-588.

Dowell C, Olivera BM, Garrett JE, Staheli ST, Watkins M, Kuryatov A, Yoshikami D, Lindstrom JM and McIntosh JM (2003) Alpha-conotoxin PIA is selective for alpha6 subunit-containing nicotinic acetylcholine receptors. *J Neurosci* **23**(24):8445-8452.

Duan Y, Wu C, Chowdhury S, Lee MC, Xiong G, Zhang W, Yang R, Cieplak P, Luo R, Lee T, Caldwell J, Wang J and Kollman P (2003) A point-charge force field for molecular mechanics simulations of proteins based on condensed-phase quantum mechanical calculations. *J Comput Chem* **24**(16):1999-2012.

Dutertre S, Nicke A and Lewis RJ (2005) Beta2 subunit contribution to 4/7 alpha-conotoxin binding to the nicotinic acetylcholine receptor. *J Biol Chem* **280**(34):30460-30468.

Dutertre S, Ulens C, Buttner R, Fish A, van Elk R, Kendel Y, Hopping G, Alewood PF, Schroeder C, Nicke A, Smit AB, Sixma TK and Lewis RJ (2007) AChBP-targeted alpha-conotoxin correlates distinct binding orientations with nAChR subtype selectivity. *EMBO J* **26**(16):3858-3867.

Ellison M, Feng ZP, Park AJ, Zhang X, Olivera BM, McIntosh JM and Norton RS (2008) Alpha-RgIA, a novel conotoxin that blocks the alpha9alpha10 nAChR: structure and identification of key receptor-binding residues. *J Mol Biol* **377**(4):1216-1227.

Ellison M, Gao F, Wang HL, Sine SM, McIntosh JM and Olivera BM (2004) Alpha-conotoxins ImI and ImII target distinct regions of the human alpha7 nicotinic acetylcholine receptor and distinguish human nicotinic receptor subtypes. *Biochemistry* **43**(51):16019-16026.

Everhart D, Reiller E, Mirzoian A, McIntosh JM, Malhotra A and Luetje CW (2003) Identification of residues that confer alpha-conotoxin-PnIA sensitivity on the alpha 3 subunit of neuronal nicotinic acetylcholine receptors. *J Pharmacol Exp Ther* **306**(2):664-670.

Gotti C, Clementi F, Fornari A, Gaimarri A, Guiducci S, Manfredi I, Moretti M, Pedrazzi P, Pucci L and Zoli M (2009) Structural and functional diversity of native brain neuronal nicotinic receptors. *Biochem Pharmacol* **78**(7):703-711.

Molecular Pharmacology Fast Forward. Published on July 16, 2012 as DOI: 10.1124/mol.112.078683
This article has not been copyedited and formatted. The final version may differ from this version.

Harvey SC, McIntosh JM, Cartier GE, Maddox FN and Luetje CW (1997) Determinants of specificity for alpha-conotoxin MII on alpha3beta2 neuronal nicotinic receptors. *Mol Pharmacol* **51**(2):336-342.

Hess B, Kutzner C, van der Spoel D and Lindahl E (2008) GROMACS 4: Algorithms for Highly Efficient, Load-Balanced, and Scalable Molecular Simulation. *Journal of Chemical Theory and Computation* **4**(3):435-447.

Hibbs RE and Gouaux E (2011) Principles of activation and permeation in an anion-selective Cys-loop receptor. *Nature* **474** (7349):54-60.

Hone AJ, Whiteaker P, Mohn JL, Jacob MH and McIntosh JM Alexa Fluor 546-ArIB[V11L;V16A] is a potent ligand for selectively labeling alpha 7 nicotinic acetylcholine receptors. *J Neurochem* **114**(4):994-1006.

Kaiser SA, Soliakov L, Harvey SC, Luetje CW and Wonnacott S (1998) Differential inhibition by alpha-conotoxin-MII of the nicotinic stimulation of [3H]dopamine release from rat striatal synaptosomes and slices. *J Neurochem* **70**(3):1069-1076.

Kim HW and McIntosh JM (2012) α6 nAChR subunit residues that confer α-conotoxin BuIA selectivity. *FASEB J*. **(in press)**

Leisgen C, Kuester M and Methfessel C (2007) The Roboocyte. *Patch-Clamp Methods and Protocols*:87-87.

Li SX, Huang S, Bren N, Noridomi K, Dellisanti CD, Sine SM and Chen L Ligand-binding domain of an alpha7-nicotinic receptor chimera and its complex with agonist. *Nat Neurosci* **14**(10):1253-1259.

Loughnan ML, Nicke A, Jones A, Adams DJ, Alewood PF and Lewis RJ (2004) Chemical and functional identification and characterization of novel sulfated alpha-conotoxins from the cone snail Conus anemone. *J Med Chem* **47**(5):1234-1241.

Mahoney MW and Jorgensen WL (2000) A five-site model for liquid water and the reproduction of the density anomaly by rigid, nonpolarizable potential functions. *The Journal of Chemical Physics* **112**(20):8910-8922.

McIntosh JM, Azam L, Staheli S, Dowell C, Lindstrom JM, Kuryatov A, Garrett JE, Marks MJ and Whiteaker P (2004) Analogs of alpha-conotoxin MII are selective for alpha6-containing nicotinic acetylcholine receptors. *Mol Pharmacol* **65**(4):944-952.

McIntosh JM, Dowell C, Watkins M, Garrett JE, Yoshikami D and Olivera BM (2002) Alpha-conotoxin GIC from Conus geographus, a novel peptide antagonist of nicotinic acetylcholine receptors. *J Biol Chem* **277**(37):33610-33615.

Nicke A, Loughnan ML, Millard EL, Alewood PF, Adams DJ, Daly NL, Craik DJ and Lewis RJ (2003) Isolation, structure, and activity of GID, a novel alpha 4/7-conotoxin with an extended N-terminal sequence. *J Biol Chem* **278**(5):3137-3144.

Nicke A, Wonnacott S and Lewis RJ (2004) Alpha-conotoxins as tools for the elucidation of structure and function of neuronal nicotinic acetylcholine receptor subtypes. *Eur J Biochem* **271**(12):2305-2319.

Olivera BM, Quik M, Vincler M and McIntosh JM (2008) Subtype-selective conopeptides targeted to nicotinic receptors: Concerted discovery and biomedical applications. *Channels (Austin)* **2**(2).

Pehl U, Leisgen C, Gampe K and Guenther E (2004) Automated higher-throughput compound screening on ion channel targets based on the Xenopus laevis oocyte expression system. *Assay Drug Dev Technol* **2**(5):515-524.

Sali A and Blundell TL (1993) Comparative protein modelling by satisfaction of spatial restraints. *J Mol Biol* **234**(3):779-815.

Taly A, Corringer PJ, Guedin D, Lestage P and Changeux JP (2009) Nicotinic receptors: allosteric transitions and therapeutic targets in the nervous system. *Nat Rev Drug Discov* **8**(9):733-750.

Tsetlin V, Utkin Y and Kasheverov I (2009) Polypeptide and peptide toxins, magnifying lenses for binding sites in nicotinic acetylcholine receptors. *Biochem Pharmacol* **78**(7):720-731.

Unwin N (2005) Refined structure of the nicotinic acetylcholine receptor at 4A resolution. *J Mol Biol* **346**(4):967-989.

Whiteaker P, Christensen S, Yoshikami D, Dowell C, Watkins M, Gulyas J, Rivier J, Olivera BM and McIntosh JM (2007) Discovery, synthesis, and structure activity of a highly selective alpha7 nicotinic acetylcholine receptor antagonist. *Biochemistry* **46**(22):6628-6638.

Whiteaker P, Marks MJ, Christensen S, Dowell C, Collins AC and McIntosh JM (2008) Synthesis and characterization of 125I-alpha-conotoxin ArIB[V11L;V16A], a selective alpha7 nicotinic acetylcholine receptor antagonist. *J Pharmacol Exp Ther* **325**(3):910-919.

Zwart R and Vijverberg HP (1998) Four pharmacologically distinct subtypes of alpha4beta2 nicotinic acetylcholine receptor expressed in *Xenopus laevis* oocytes. *Mol Pharmacol.* **54**(6):1124-31.

Molecular Pharmacology Fast Forward. Published on July 16, 2012 as DOI: 10.1124/mol.112.078683
This article has not been copyedited and formatted. The final version may differ from this version.

Footnotes

These Authors contributed equally to the work: Mirko Beissner, Sébastien Dutertre, Rudolf Schemm. This work was supported by the Deutsche Forschungsgemeinschaft [Grants NI 592/3 and 592/5]

Molecular Pharmacology Fast Forward. Published on July 16, 2012 as DOI: 10.1124/mol.112.078683
This article has not been copyedited and formatted. The final version may differ from this version.

Figure Legends

FIGURE 1. Sequence alignment. Rat α4 and α3 nAChR subunits have 61.84 % sequence identity in their ligand binding domain. Asterisks indicate the position of residues mutated in this study.

FIGURE 2. Agonist dose response curves for ACh. The indicated wt and mutant α3 and α4 subunits were coexpressed with β2 subunits in *Xenopus laevis* oocytes. Responses to ACh were measured at –60 mV with the Roboocyte™ system or at -70 mV with a conventional TEVC setup (red lines and symbols, control experiments for the most critical mutants in this study). Dose response curves for (A) wt and mutant α3β2 and α4β2 receptors and (B) different α4β2 mutants.

FIGURE 3. Concentration-response analysis of α-conotoxins MI, TxIA, and [A10L]TxIA on wild type and mutant nAChRs. The indicated subunit combinations were expressed in *Xenopus* oocytes and analyzed by 2-electrode voltage clamp. Responses to 2-s pulses of 100 μM ACh were recorded after a 3-min preincubation with the indicated toxin. IC_{50} values and Hill slopes are given in Table 2. Each point represents the average of at least 4 measurements. Error bars represent S.E. The dotted line in (E) shows the same data as in (D).

FIGURE 4. Molecular simulations of conotoxin binding in wt and mutant α4β2 homology models. (A) Position of TxIA in the binding site of α4β2 based on the co-crystal structure with AChBP, showing the absence of a steric clash between the conotoxin and receptor residues. The model of the α4β2 receptor was generated using the AChBP bound to TxIA crystal structure as a template, as previously described (Dutertre et al., EMBO J, 2007) (B) Loops C of wt α4 subunit

Molecular Pharmacology Fast Forward. Published on July 16, 2012 as DOI: 10.1124/mol.112.078683
This article has not been copyedited and formatted. The final version may differ from this version.

models based on AChBP (orange) and *T. torpedo* nAChR (yellow) with the respective TxIA (starting structures). (C, D, E) Loops C of wt (yellow), α4(R185I)β2 (green), α4(P195Q)β2 (cyan), and α4(R185I, P195Q)β2 (magenta) receptor models based on the *Torpedo* nAChR with the [A10L]TxIA conotoxin in minimized average structures.

FIGURE 5. Calculated average [A10L]TxIA α-conotoxin distances and binding enthalpies. (A) α-Conotoxin distances to loop C (R(I)185-Y194) of α4 (orange) and to β2 subunit (center of mass of backbone) (green). (B) Binding enthalpies (sum of short-range Coulomb+Lennard-Jones energies) for α-conotoxin [A10L]TxIA with wt, P195Q, R185I, and P195Q/R185I α4 subunits (red) and with β2 subunits (green). Overall binding energies are shown in blue. Energies and distances were calculated from 10 to 50 ns.

Molecular Pharmacology Fast Forward. Published on July 16, 2012 as DOI: 10.1124/mol.112.078683
This article has not been copyedited and formatted. The final version may differ from this version.

Tables

TABLE 1. EC_{50} values for acetylcholine at wt and mutant α3β2 and α4β2 receptors obtained with the robocyte system. Hill coefficients were constrained between 0 and 2 in cases where the originally obtained coefficients were unreliable (CI > 4). For comparison, asterisks represent values obtained in a conventional TEVC set up.

	EC_{50} [μM]	95% CI	Hill Slope
α3β2	369.6	302-453	0.9
α3(I186R)β2	376.7	313-454	1.0
α4β2	91.9/93.9*	76-111/76-117*	2.0/1.9*
α4(T147S)β2	75.2	44-128	2.0
α4(A191E)β2	87.3	67-113	2
α4(E188N)β2	56.7	46-71	1.0
α4(R185I)β2	108.9/138.0*	88-135/115-166*	2.0/1.8*
α4(R185A)β2	61.4	45-84	1.3
α4(R185K)β2	139.8	91-214	2.0
α4(R185E)β2	80.3	52-125	2.0
α4(P195Q)β2	66.5/110.5*	37-120/43-282*	1.2/0.7*
α4(P195Q/R185I)β2	7.3/5.6*	3.2-16.4/3.6-8.7*	1.1/0.8*

Molecular Pharmacology Fast Forward. Published on July 16, 2012 as DOI: 10.1124/mol.112.078683
This article has not been copyedited and formatted. The final version may differ from this version.

TABLE 2. IC_{50} values and Hill coefficients (nH) for the α-conotoxins MII, TxIA, and [A10L]TxIA at wt and mutant α3β2 and α4β2 receptors. Numbers in brackets represent 95% confidence intervals.

	MII		TxIA		[A10L]TxIA	
	IC_{50} [nM]	n_H	IC_{50} [nM]	n_H	IC_{50} [nM]	n_H
α4β2	3293 (2855-3798)	-0.852	–	–	–	–
α4(T147S)β2	3206 (2538-4050)	-0.903	–	–	n.d.	–
α4(E188N)β2	3766 (3253-4361)	-1.03	–	–	n.d.	–
α4(A191E)β2	1938 (1683-2233)	-0.996	–	–	n.d.	–
α4(R185I)β2	192.8 (158-236)	-1.058	18.1 (15.2-21.6)	-0.813	123 (102-113)	-0.835
α4(R185A)β2	n.d.	–	n.d.	–	415	-0.980

Molecular Pharmacology Fast Forward. Published on July 16, 2012 as DOI: 10.1124/mol.112.078683
This article has not been copyedited and formatted. The final version may differ from this version.

					(333-515)	
α4(R185K)β2	n.d.	–	n.d.	–	–	–
α4(R185E)β2	n.d.	–	n.d.	–	91.8 (74.8-113)	-1.079
α4β2V109G)	n.d.	–	n.d.	–	213 (167-271)	-1.031
α4(R185I) β2(V109G)	n.d.	–	n.d.	–	6.6 (4.8-9.1)	-0.755
α4(P195Q)β2	n.d.	–	n.d.	–	707 (533-939)	-0.88
α4(R185I,P195) β2	n.d.	–	n.d.	–	3.2 (2.6-3.8)	-1.11
α3β2	4.2	-0.887	2 (1.68-2.43)	-1.062	2.0 (Dutertre et al., 2007) (1.8–2.4)	-
α3(I186R)β2	58.3 (45.1-75.5)	-1.327	60.4 (50.9-71.6)	-1.033	76.5 (58.9-99.3)	-1.261

Molecular Pharmacology Fast Forward. Published on July 16, 2012 as DOI: 10.1124/mol.112.078683
This article has not been copyedited and formatted. The final version may differ from this version.

TABLE 3. Sequence comparison of the 4/7 α-conotoxins. Grey shading indicates residues that are generally conserved. 2/8 and 3/16 cysteine pairs form disulfide bridges.

	1 2 3 4 5 6 7 8 9 10 11 12 13 14 15 16
MII	**G C C** S N **P** V **C** H L E H S N L **C**
TxIA	**G C C** S R **P** P **C** I A N N P D L **C**
[A10L]TxIA	**G C C** S R **P** P **C** I L N N P D L **C**
PnIA	**G C C** S L **P** P **C** A A N N P D Y **C**
EpI	**G C C** S D **P** R **C** N M N N P C Y **C**
GID	**I R D γ C C** S N **P** A **C** R V N N O H V **C**

Figure 1

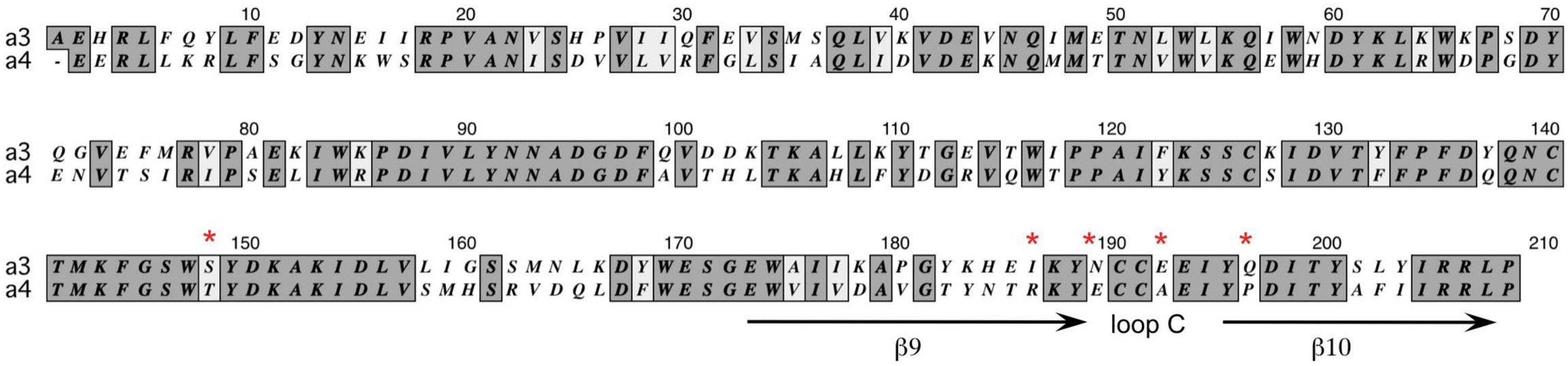

Molecular Pharmacology Fast Forward. Published on July 16, 2012 as DOI: 10.1124/mol.112.078683
This article has not been copyedited and formatted. The final version may differ from this version.

Figure 2

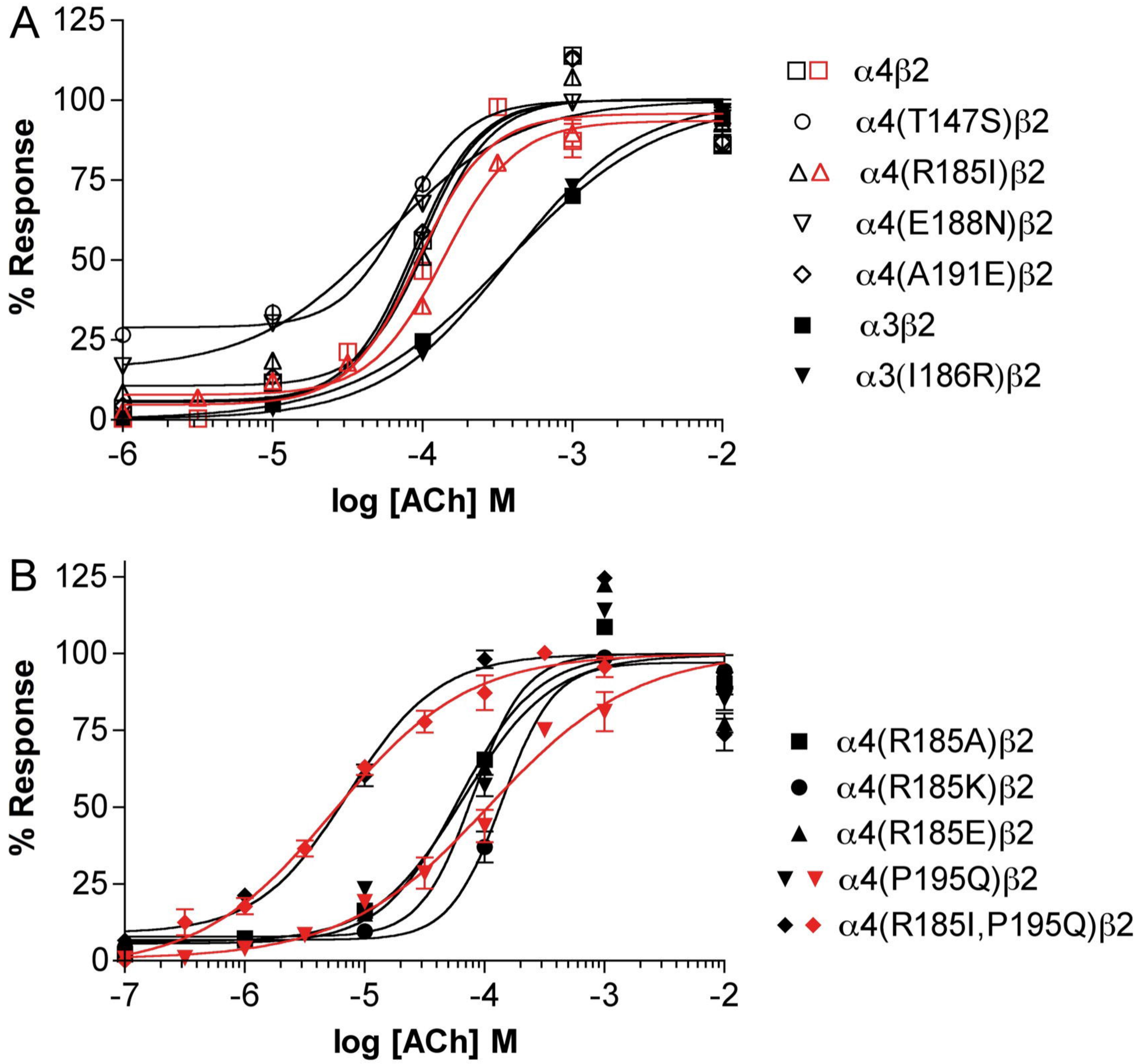

Molecular Pharmacology Fast Forward. Published on July 16, 2012 as DOI: 10.1124/mol.112.078683
This article has not been copyedited and formatted. The final version may differ from this version.

Figure 3

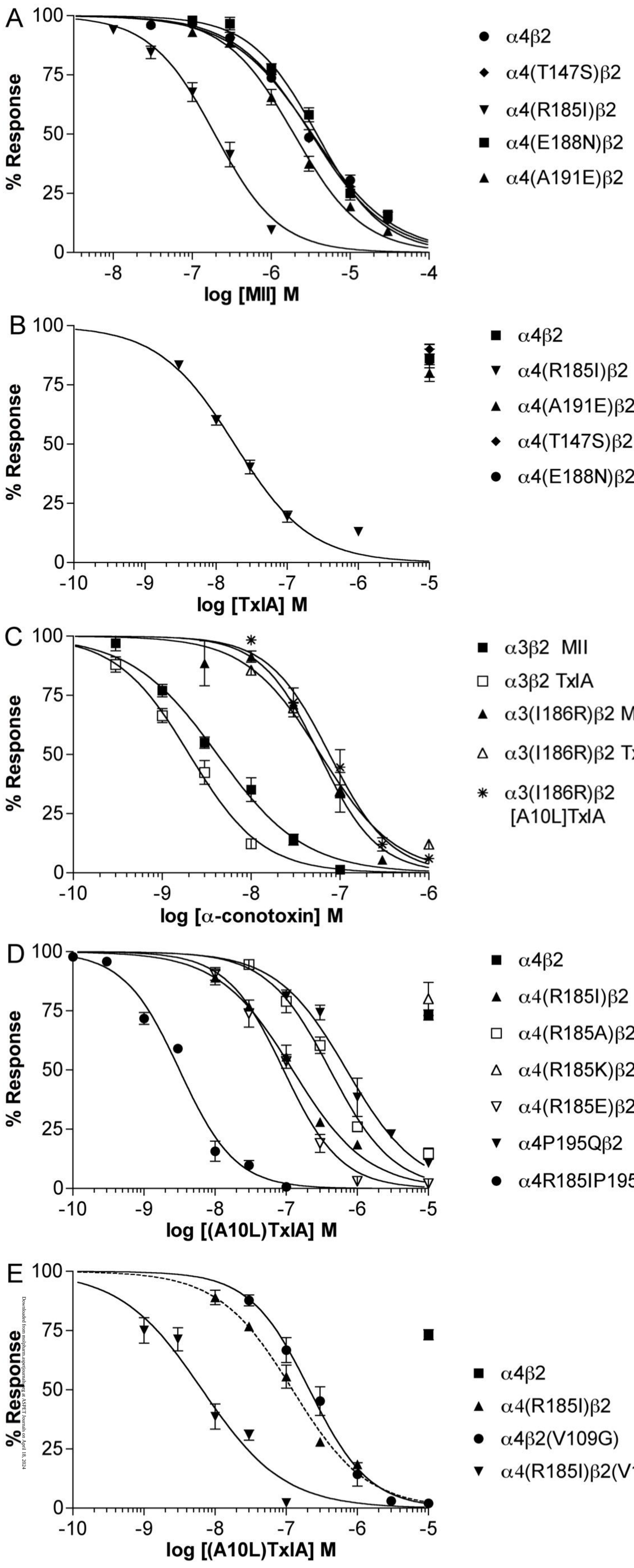

Molecular Pharmacology Fast Forward. Published on July 16, 2012 as DOI: 10.1124/mol.112.078683
This article has not been copyedited and formatted. The final version may differ from this version.

Figure 4

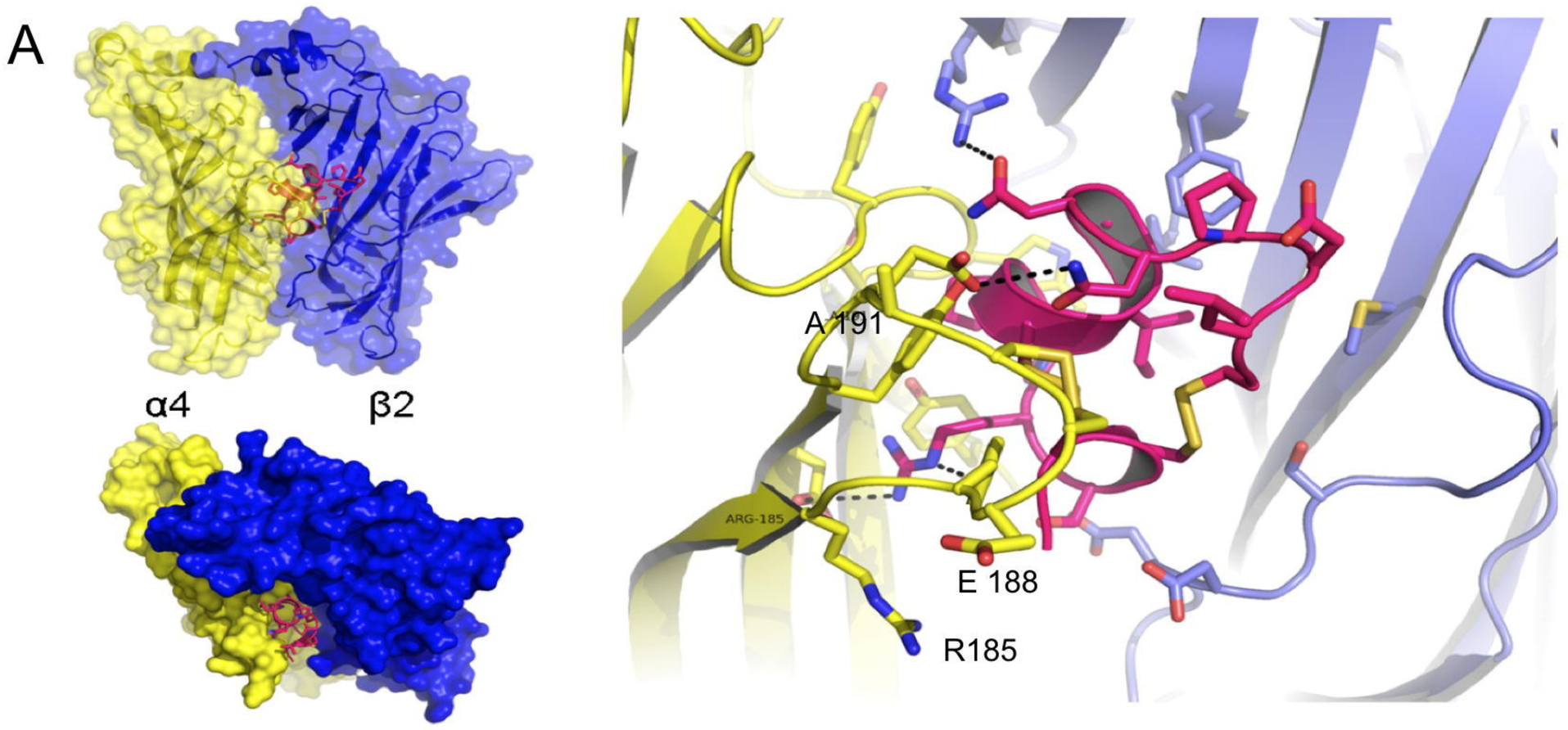

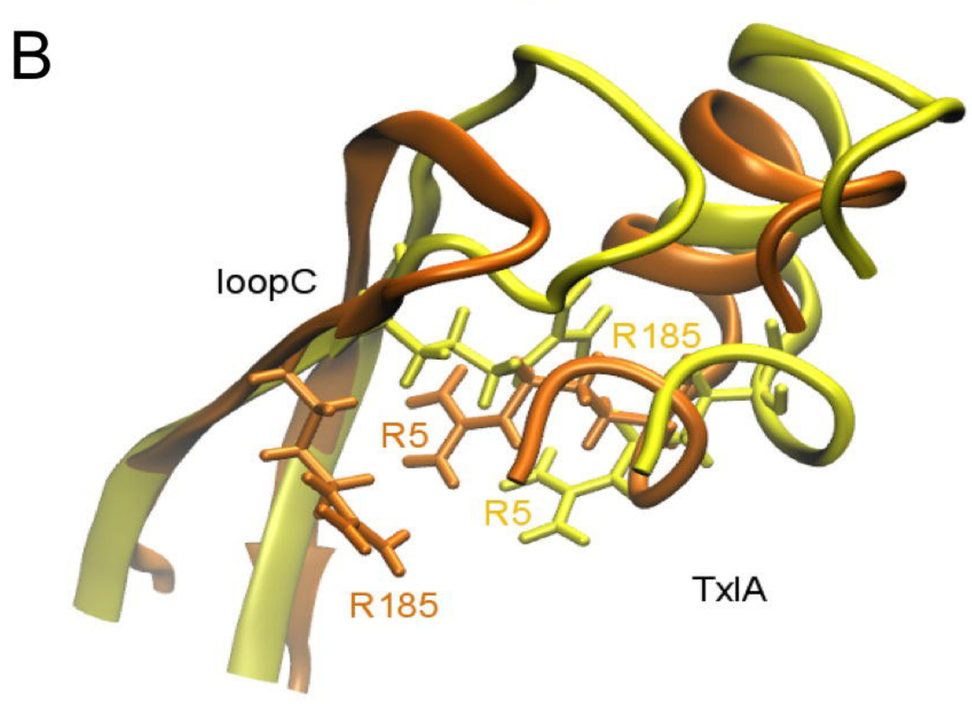

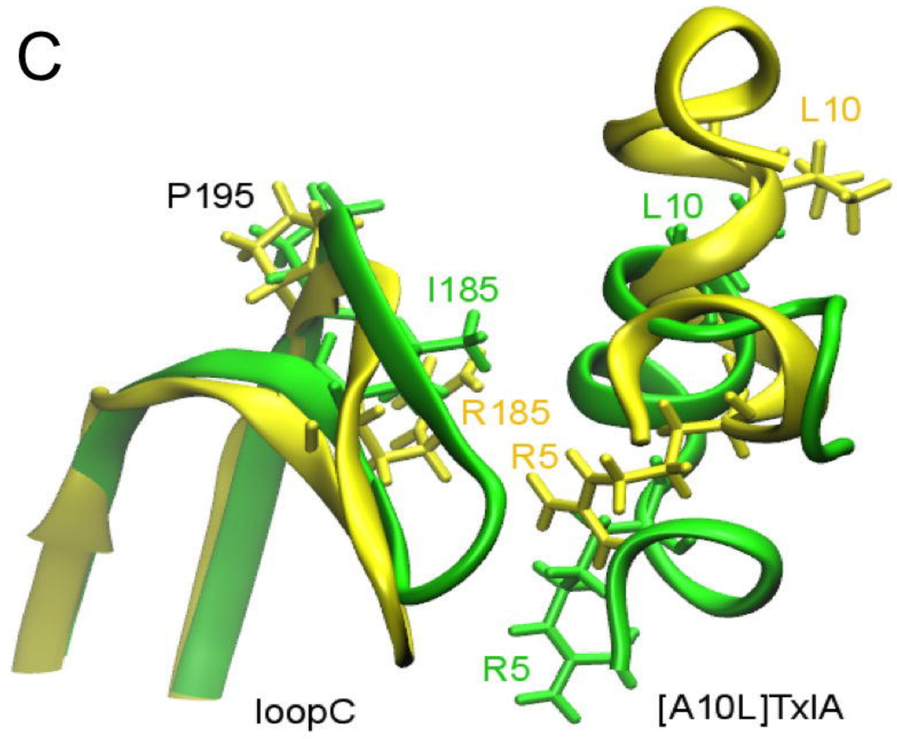

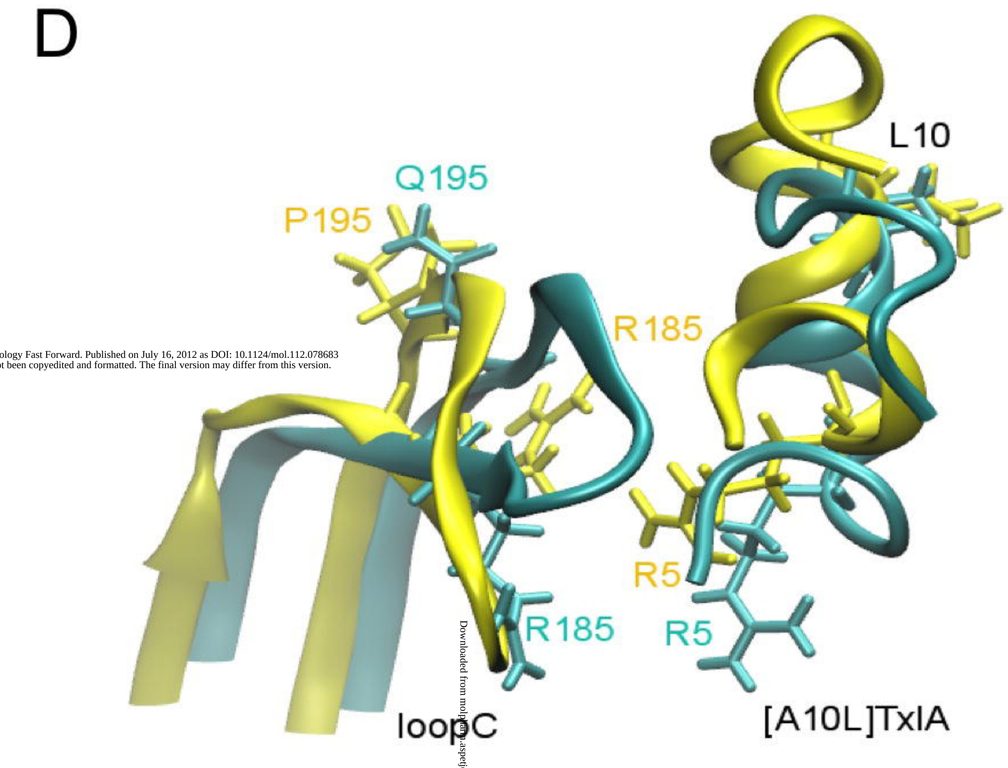

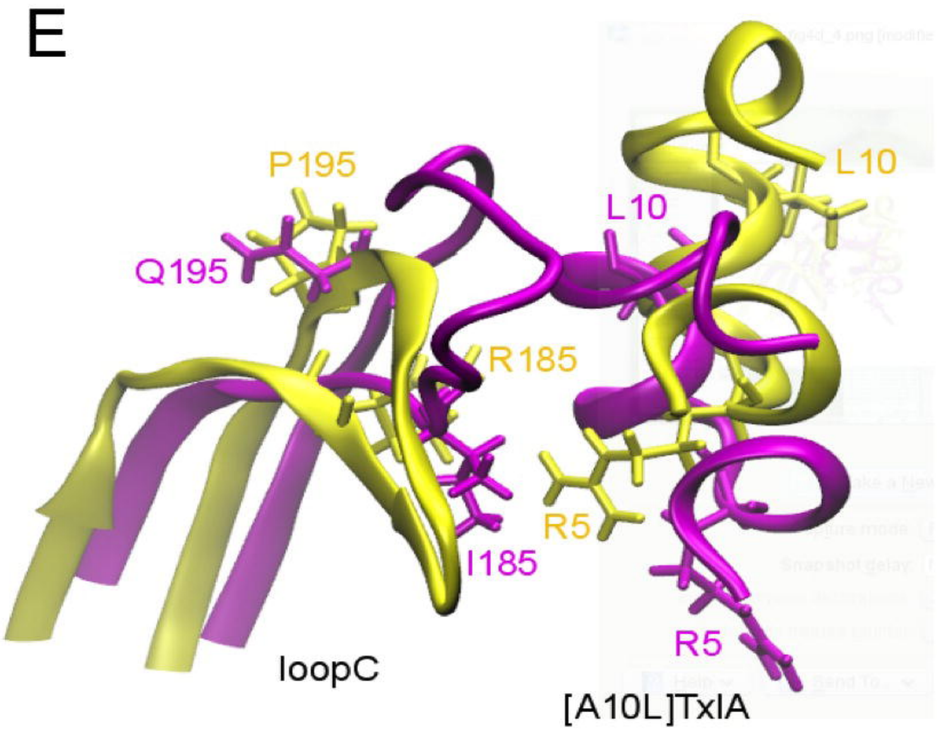

Molecular Pharmacology Fast Forward. Published on July 16, 2012 as DOI: 10.1124/mol.112.078683
This article has not been copyedited and formatted. The final version may differ from this version.

Figure 5

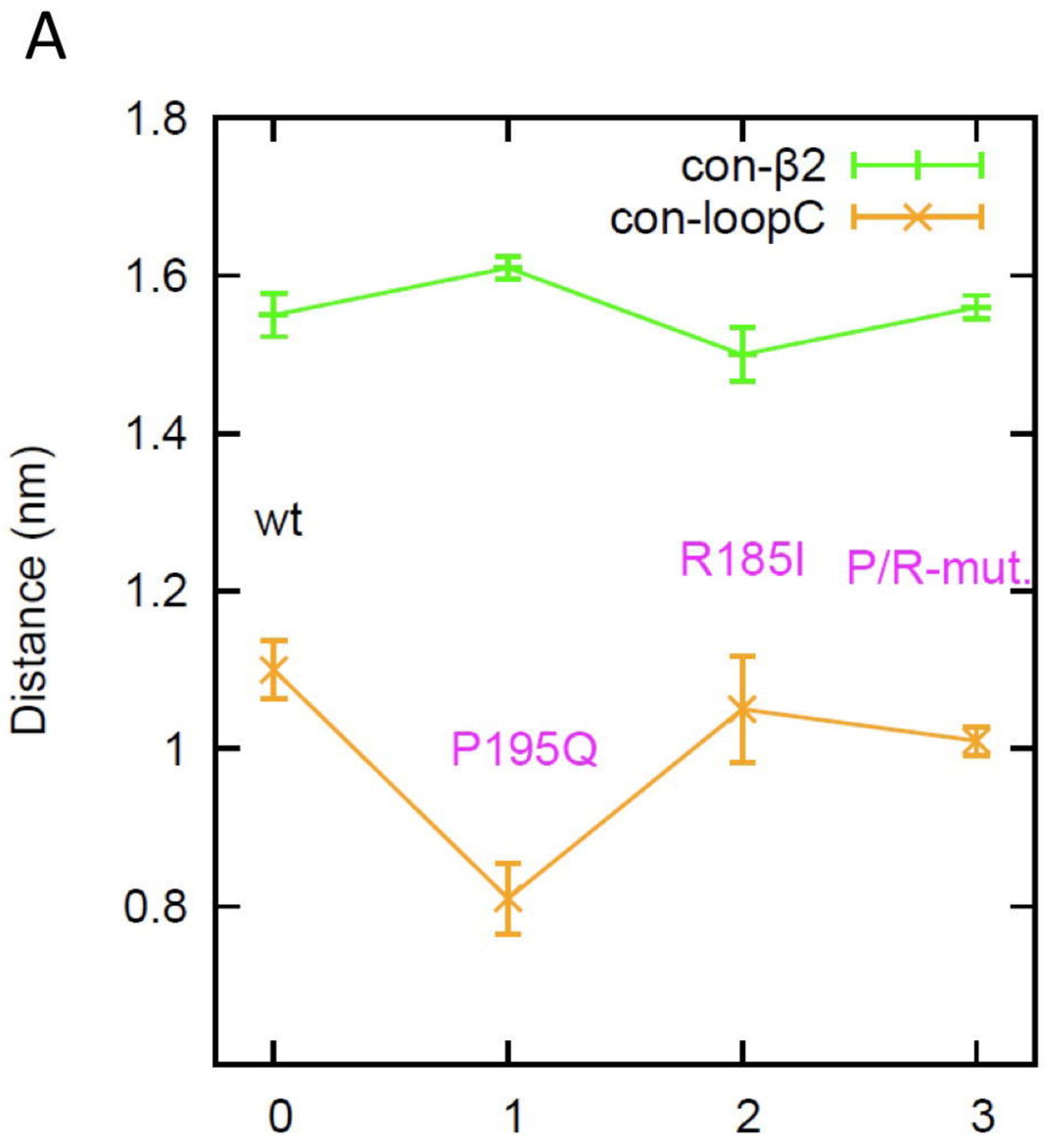

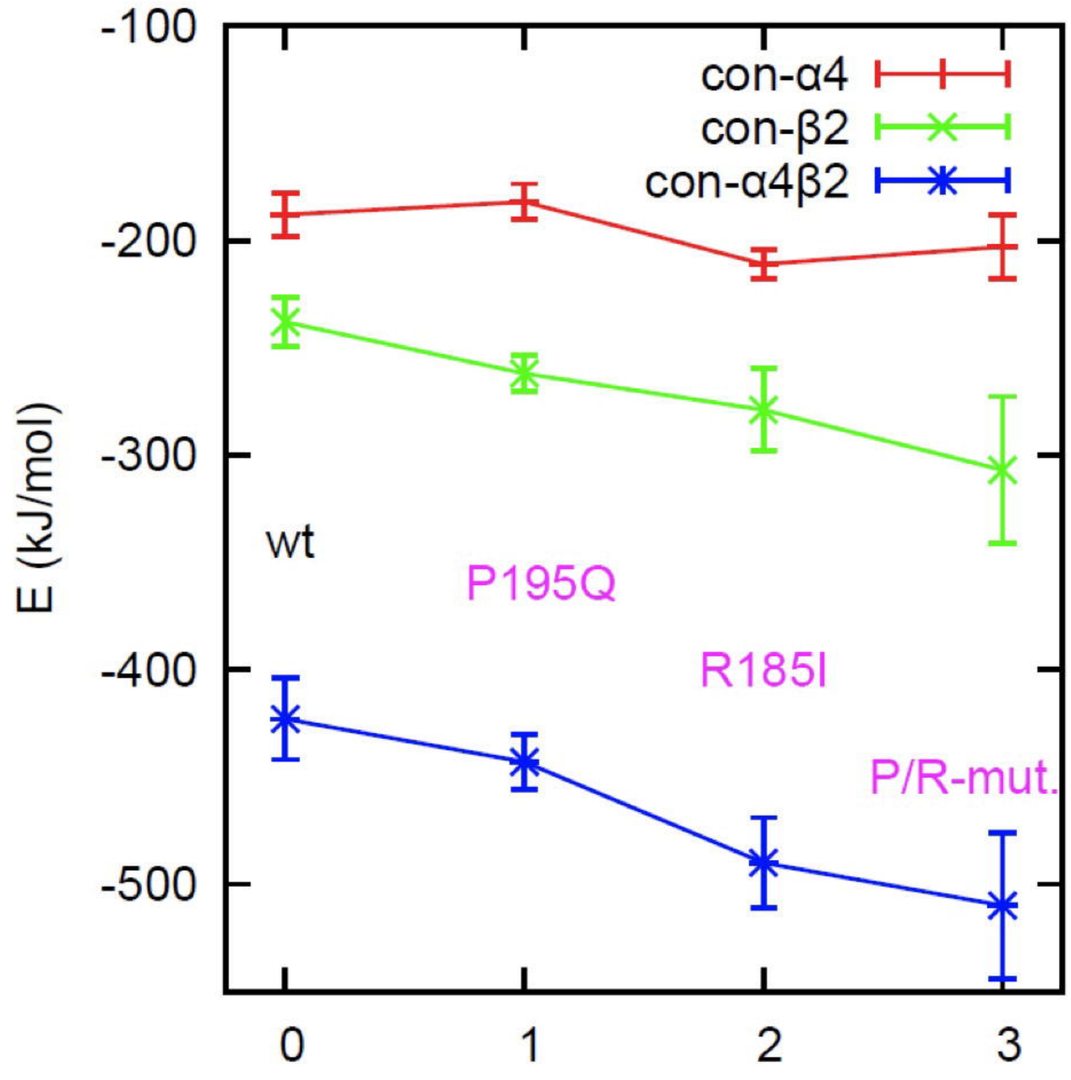

Molecular Pharmacology Fast Forward. Published on July 16, 2012 as DOI: 10.1124/mol.112.078683
This article has not been copyedited and formatted. The final version may differ from this version.

Efficient binding of 4/7 α-conotoxins to nicotinic α4β2 receptors is prevented by R185 and P195 in the α4 subunit

Mirko Beissner*, Sébastien Dutertre*, Rudolf Schemm*, Timm Danker, Annett Sporning, Helmut Grubmüller, and Annette Nicke

Molecular Pharmacology

Supplemental Information:

Bayesian analysis

To determine the statistical significance of the observed enthalpy trend, we have assumed that this trend is described by the linear function $E_j = mj + b$, where j=0,1,2,3 labels the four systems wt, P195Q, R185I, and R185I, P195Q, respectively, and the E_j denote the respective interaction enthalpies. We have then calculated the conditional probability for the slope m and the offset b for given enthalpies E_j and their standard deviations σ_j via Bayes' formula,

$$p(m, b|\{E_j, \sigma_j\}_{j=0,1,2,3}) \propto p(\{E_j\}_{j=0,1,2,3}|m, b, \{\sigma_j\}_{j=0,1,2,3}) \cdot p(m, b)$$

where the right side term describes that reverse conditional probability

$$p(\{E_j\}_{j=0,1,2,3}|m, b, \{\sigma_j\}_{j=0,1,2,3}) = \prod_{j=0}^{3} \exp\left[\frac{-(mj + b - E_j)^2}{2\sigma_j^2}\right]$$

that the four enthalpies are obtained for *given statistical accuracies* σ_j , slope *m* and offset *b*, times the *a priori* probability distribution for *m* and *b*, which we assume to be uniformly distributed. Numerical integration over *b* and proper normalization yields the bell-shaped *a posteriori* probability distribution for *m*, given the enthalpies determined from the MD simulation,

$$p(m|\{E_j, \sigma_j\}_{j=0,1,2,3}) = \frac{\int_{-\infty}^{\infty} db\, p(m, b|\{E_j, \sigma_j\}_{j=0,1,2,3})}{\int_{-\infty}^{\infty} db \int_{-\infty}^{\infty} dm\, p(m, b|\{E_j, \sigma_j\}_{j=0,1,2,3})}$$

From this *a posteriori* probability distribution, one readily obtains the probability that *m* is negative,

$$p(m < 0) = \int_{-\infty}^{0} p(m)dm \approx 0.9986,$$

which implies a significance level of 1-0.9986 = 0.14%.

Supplemental Figure 1

A

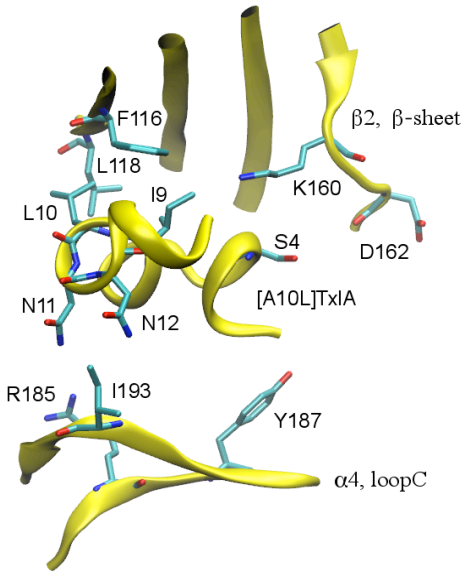

B

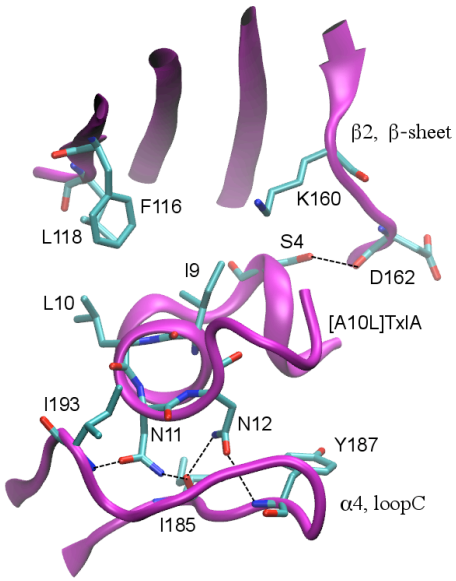

Fig. S1: Top view of minimized conotoxin average structures showing [A10L]TxIA bound to wt α4β2 (A) and α4(R185I,P195Q)β2 (B) nAChR receptor models (*Torpedo* nAChR-based models). Note that in the wt, S4, N11, and N12 do not directly interact with the α4 and β2 subunits, whereas in the α4(R185I, P195Q)β2 mutant these residues interact closely with the respective subunits forming an H-bonding network (dashed lines). Thus, the critical mutations R185I and P195Q (not shown) allow a much more favorable positioning of the conotoxin and a better adaption of loop C to it.

Supplemental Figure 2

To test the suitability of both α4β2 nAChR models, the rmsds of their loops C were analyzed for the wt proteins. The low values obtained for the AChBP-based model compared to the *Torpedo* nAChR-based model, suggest that in the first model, loop C is almost unaffected by the docked contoxin. As expected from the experimental results, considerable structural rearrangements take place in loop C of the *Torpedo*-based model.

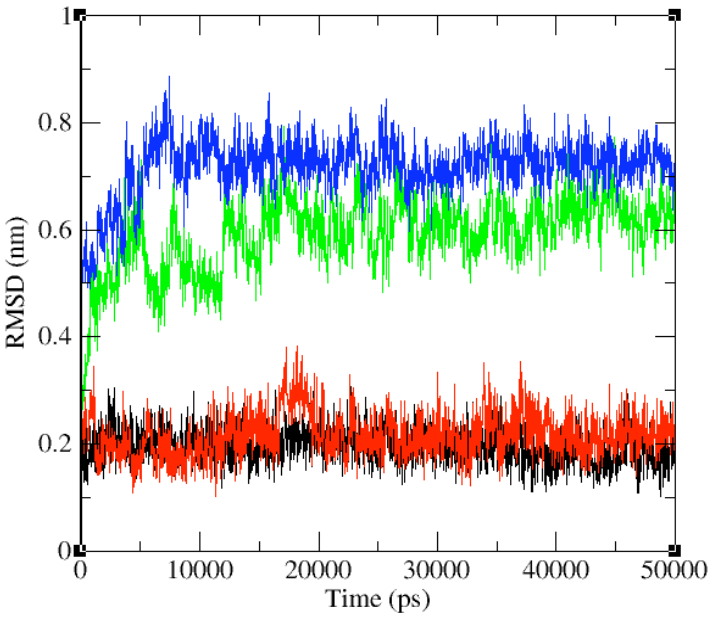

Fig. S2: RMSD values of loops C, relative to the conotoxin backbone in MD simulations with the AChBP-based model (black and red) and in two representative runs with the *Torpedo marmorata* nAChR-based model (green and blue).

In addition, the alteration of the loop C - conotoxin interaction by mutations was calculated. RMSD values (averaged from 8-10 simulations) for loops C (fitted to conotoxin) in wt (0.59 nm) and P195Q mutated proteins (0.57 nm) show the largest loop C changes, followed by the double mutant R185I, P195Q (0.37 nm). A single R185I exchange results in the lowest value (0.30 nm). This documents the influence of R185 on conotoxin binding.

Supplemental Figure 3

In order to detect interactions of loop C residues with the [A10L]TxIA conotoxin that could account for the different overall energies (see Fig. 5), we calculated the respective interactions from four MD simulations of each protein/conotoxin combination.

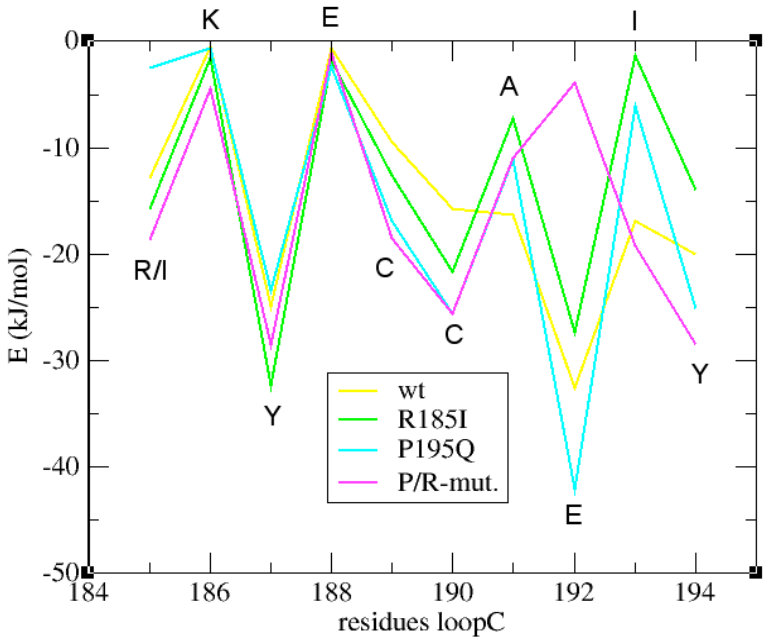

Fig. S3: Interaction energies of loop C residues of differently mutated proteins to the docked conotoxin [A10L]TxIA. For wt, R185I, P195Q, and R185I/P195Q mutations, values of 129.9, 121.7, 130.7, and 131.1 kJ/mol (sum of single interactions) were obtained, respectively.
Surprisingly, these energies do not strictly correlate with the measured overall energies (see Fig. 5) and moreover, the energies per protein/conotoxin combination do not differ significantly, suggesting that the overall energies detected for differently mutated proteins cannot be ascribed to specific conotoxin-loop C residue interactions. This is especially true for the R185I mutation.

Supplemental Figure 4

To illustrate how loops C of the different mutations overlap in MD simulations and where the largest fluctuations occur, we plotted their ribbons in varying thickness. Unexpectedly, the extent of residue fluctuations seems to be independent of the mutation. This suggests a common inherent behavior of all loops C.

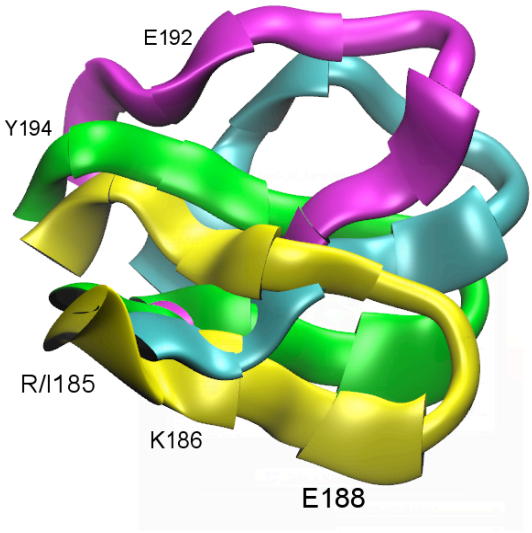

Fig. S4: Loops C conformations in minimized average structures of wt (yellow), α4(R185I)β2 (green), α4(P195Q)β2 (cyan), and α4(R185I, P195Q)β2 (magenta) receptor models based on the *Torpedo* nAChR with the [A10L]TxIA conotoxin. Line width corresponds to average RMSF values for each residue with thin ribbon (low fluctuation) to thick ribbon (high fluctuation). Average rmsf values: R/I185: 0.16 nm ~ E188: 0.16 nm > K186: 0.15 nm > E192 0.13 nm > Y194: 0.12; others below 0.1 nm (highest values for single residues: R185 (wt) 0.24